



# Key Technologies for the Cushion Cap Construction of the Longshan Highway Bridge

Yuan Yin, Dengwu Li, Yin He, Shufan Cheng\*

Hubei Province Road and Bridge Co. Ltd., 38# Dongfeng Avenue, Wuhan, Hubei 430056, China

\*Email: chengshufan@whu.edu.cn

**Abstract.** Longshan Bridge is located on the mainstream of the Han River in the Danjiangkou Reservoir. The main bridge takes a 6-span prestressed concrete continuous beam with a solid pier and bored piles as the foundation. The construction of piers 7 #~9 # of the main bridge, which are far away from the riverbank, adopts the scheme of first boxed cofferdam and then pile. In this scheme, the zone of the boxed cofferdam was located by the positioning device on the nearby completed pier, and the boxed cofferdam was installed. Then, the new piles were derived by a vibration hammer combined with a floating sleeve. The concrete volume for a pier is 4937.52m<sup>3</sup>, which makes the temperature hard to control during the pouring process. Therefore, the water cycle pipe system is used for mass concrete cooling, and thermal destruction is almost eliminated because of the reasonable pipeline distribution. In this paper, the double-wall steel boxed cofferdam technology and concrete temperature control technology for the large-volume cushion cap were introduced. Then, by combining numerical simulation and on-site monitoring, the key points of such technology were analysed and discussed.

**Keywords:** beam bridge, massive concrete, double-wall steel boxed cofferdam

## 1 Introduction

The building of bridges, even the traditional continuous beam bridges, faces many difficulties due to its challenging construction environment, such as deep water [1-3], large spans [4,5], and complex shapes. For the substructure, the cofferdam and the large-volume concrete cushion cap construction are two key points.

In terms of the cofferdam construction, structural selection, assembly, and transportation received scholars' attention and were taken seriously. ZHU and ZHANG [6] take steel boxed cofferdam as an example, a structural safety model was proposed. WANG, etc [7] take offshore artificial island cofferdam as an example, evaluating the construction scheme. In terms of large-volume concrete pouring technology, temperature control and crack control may be important [8,9]. Longshan Bridge, a beam bridge located inside the reservoir, is a good case for bridge construction technology analysis.

In this paper, the project overview was given in section 2. In sections 3 and 4, the 3. double-wall steel boxed cofferdam technology and large volume concrete temperature

control technology were introduced respectively, which include the construction scheme and numerical simulation. Finally, concluding remarks are given in Section 5.

## 2 Project Overview

As shown in Fig. 1, Longshan Bridge is located on the mainstream of the Han River, 30 km from the Danjiangkou dam. It connects Liangshuihe Town (North) and Longshan Town (South).



**Fig. 1.** The substructure construction of Longshan Bridge

The bridge is a 6-span, prestressed concrete continuous beam system. The two side spans are 75m, and the four middle spans are 130m. The width of the bridge deck is 24.5m, which can be designed as a two-way, four-lane road. The substructure of the bridge adopts solid piers and bored piles. The connection structure adopts gravity-type U-shaped abutments.

Danjiangkou is located in the west of Hubei province, which belongs to the subtropical monsoon climate. The average annual temperature of the bridge location is between 14.3 °C and 15.9 °C, and the average annual precipitation is between 750 mm and 900 mm. Construction cannot be carried out during the rainy season from July to September.

The surface water of the construction area mainly stems from the Danjiang reservoir (the dam located north of the bridge). Affected by the cycle of the dry and flood season in the upstream zone, the water level of the reservoir varies ranging from 138.5 to 151.5 meters (In the last years). During the hydrogeological survey, the reservoir water level was 140.7m (China Yellow Sea height datum, the same below).

Along the bridge, the Middle Proterozoic Wudang Group ( $P_1^{wd}$ ) and Quaternary (Q) sedimentary layers are distributed. The lithology is distributed as follows, from old to new. (1) Strong weathered sericite quartz schist ( $P_2^{wd}$ ), (2) Moderate weathered sericite quartz schist ( $P_2^{wd}$ ), (3) Quaternary soil (including updated layer ( $Q_2^{al}$ ), Holocene layer ( $Q_4^{al}$ ,  $Q_4^{cl+dl}$  and  $Q_4^{pl+dl}$ )).

## 3 Double-Wall Steel Boxed Cofferdam Technology

### 3.1 Construction Method

The 6 # to 10 # piers foundation of the main bridge of Longshan bridge are constructed by double-wall steel boxed cofferdam construction method. The main waterway is located between #7 and #8 piers. Each pier has an independent platform, which provides a place for large equipment operation and has the same No. As the pier. There are two driving wharves (4m wide) connected to platform 10# to the north bank and platform 6# to the south bank. Platform #7 is connected to platform #6 by a walking wharf (1.2m wide). Platform #8 connected to platform #9 and continued to platform #10 by another walking wharf.

By this method, the construction of the pier cap takes in the order of pile foundation first and then boxed cofferdam. First, the wharf was set up and a platform for the pile foundation was constructed. Then, the double-wall steel boxed cofferdam was transported to and assembled at the location, after the pile foundation construction was complete. Finally, the cushion cap was constructed.

The equipment and materials are difficult to transport to the 7 #~9 # piers platform, which is in the middle of the river and the wharf is not wide enough. Therefore, the steel boxes were assembled at the dock and moved by floating transportation. In terms of this engineering, the construction process of the double-wall steel-boxed cofferdam can be conducted as follows.

**Location of the boxed cofferdam:** According to the design drawings, install temporary hanging devices on the top of the pier. The installation system is formed by 5 hanging points equipped with one 200t hydraulic jack. Preliminary positioning of the cofferdam was achieved by the installation system, and the steel casing of the pile was inserted (Fig. 2).

**Position of the boxed cofferdam:** As the steel casing insertion work is finished, the pile construction shall be carried out as continues. Each cushion cap has 8 piles as a foundation. As all piles were formed, new beams at the top of the casing were installed. The hanging points were changed to the new beams. At this moment, the located boxed cofferdam still floats on the water's surface. Then, water was symmetrically pumped into the inside space of the cofferdam which may be smoothly lowered to the design elevation (+145.0m).

**Bottom sealing of the boxed cofferdam:** After the cofferdam is lowered into place, the gaps in the bottom are sealed by steel plates, and 5m high concrete is poured. The top elevation of the sealed concrete is +150.0m. Then, the water inside of the cofferdam was pumped out, and the waste such as mud and debris concrete was removed. Finally, reinforcement was planted at the sealed concrete, and new concrete was poured to +156.5m, which is the designed elevation of the up face of the cushion cap.



Fig. 2. Location of the boxed cofferdam

### 3.2 Design and Numerical Analysis

According to the construction schedule and the actual situation on site, the top elevation of the double-wall steel-boxed cofferdam was determined to be +165.5m. The bottom elevation and the water level are set at +144.5m and +164.5m, respectively. The sectional shape of the cofferdam is octagonal, with a length of 27.3m, a width of 23.2m, a wall thickness of 1.6m, and a height of 21m (Fig.3).

The cofferdam is divided into two sections for processing, the first section is 16m and the second section is 5m, both of which are completed at the shipyard. The pile is far away from the land, therefore, a scheme first boxed cofferdam and then a pile was chosen (Fig. 4).

Once the blocks of cofferdam were transported to the platform, the structure was assembled. Then, it slides and is lowered into the water. Finally, the whole cofferdam floats to the pier position and sinks to the design elevation. After the cofferdam is in place, the pile construction will be carried out. To ensure the reliability of the design scheme, numerical simulations were conducted.

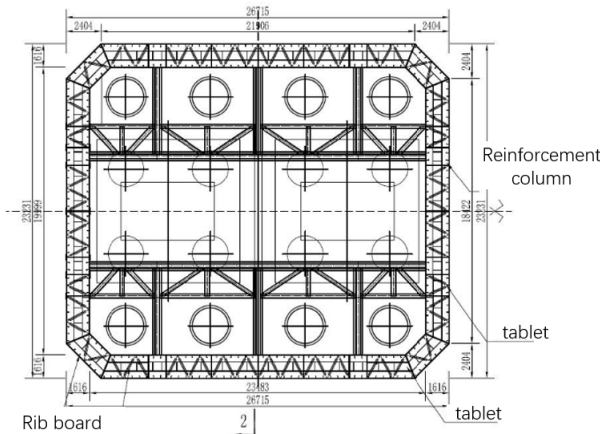
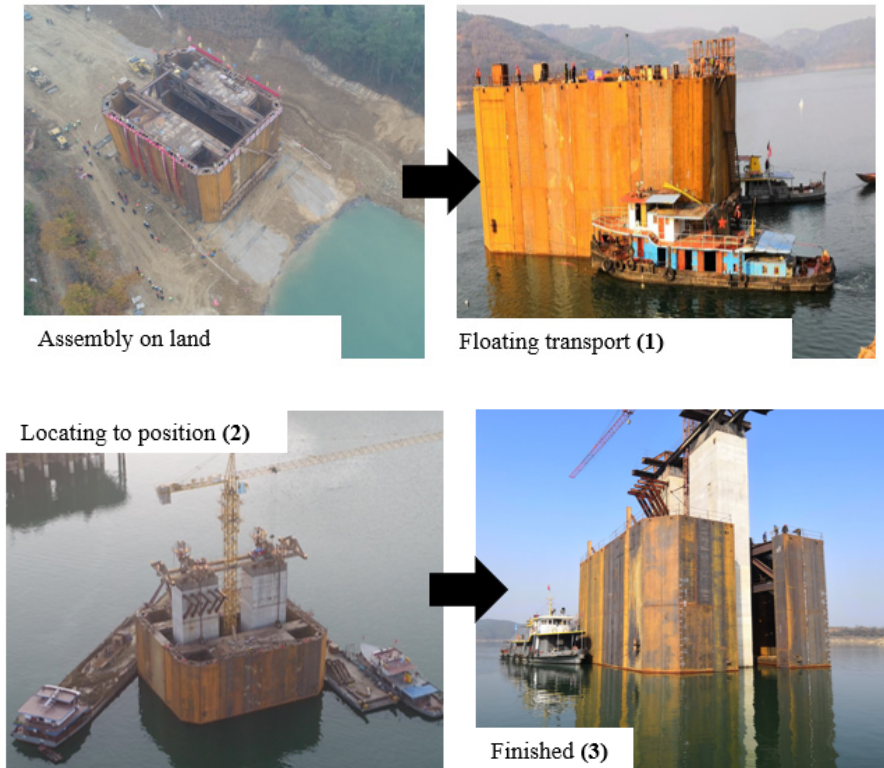


Fig. 3. Structure and layout of double arm steel sleeve box



**Fig. 4.** First boxed cofferdam and then pile scheme.

Numerical models are established and solved using Midas Civil, which is a reliable general software. The numerical model is shown in Fig. 5, and the cross-sectional and section characteristics of the components are shown in Table 1.

**Table 1.** Section characteristics of components

Component	Model (cross-sectional size) /mm	$A$	$I_x$	$W_x$
		cm <sup>2</sup>	cm <sup>4</sup>	cm <sup>3</sup>
vertical rib	bulb flat steel (160×80)	16.2	411	43.3
horizontal brace	square steel (B120×8)	19.2	696.6	116.1
inter-support (beam)	double flange beam (1000×600×20×25)	720	944960	18899
inter-support (truss)	flange beam (HM588×300×12/20)	187.2	114350	3890

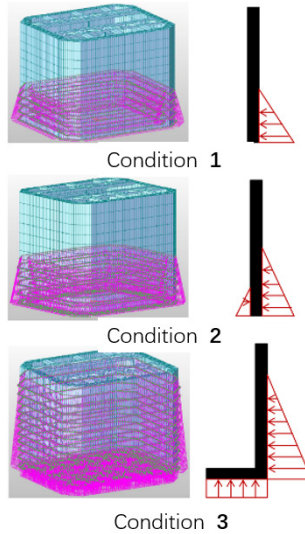


**Fig. 5.** Model of double-arm steel sleeve box

As shown in Fig. 5, three working conditions are mainly considered, which can reflect the real construction process. Work condition 1 corresponds to the double-wall steel boxed cofferdam staying at the draft depth, which checks the stress and deformation during the floating process. The cofferdam is 21 meters high, and a part of it sinks into the water due to its weight. The water depth is 7.5m, and the top elevation of the cofferdam is +179.75. There is no water in the cofferdam, and the inside and outside water head difference will cause the cofferdam to bear hydrostatic pressure. The verification results are shown in the following Fig. 6-(a) and Table 2.

Work condition 2 corresponds to the cofferdam's stay at the designed elevation, in which water has already been injected into the box. The design water level is +165.5m, therefore the cofferdam still needs to sink 1.95m. At this time, 277.1t water will be injected, and the water level outside the wall compartment will increase to 8.7m high. The verification results are shown in the following Fig. 6-(b) and Table 3.

Work condition 3 corresponds to the bottom concrete being completed, and water being pumped out. This condition can be used for checking the thickness of the bottom concrete and the anti-floating calculation of the cofferdam. In this condition, the water level outside is 20m, which is determined by available hydrological data. The verification results, including the anti-floating and anti-sliding verification, are shown in the following Fig. 6-(c) and Table 4.

**Table 2.** Verification results of work condition 1

Component	Normal stress /(MPa)	Shearing stress /(MPa)	Displacement /(mm)
vertical rib	151.6	0.41	0.26
horizontal brace	85.8	3.4	0.31
inter-support	32.2	18.6	0.34

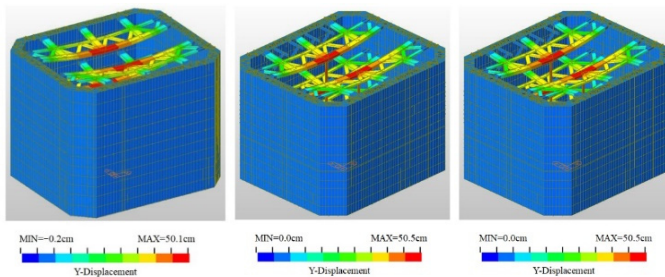
(beam)			
inter-support	65.3	6.0	50.1
(truss)			
<b>Maximum displacement</b>		<b>50.1 cm</b>	
<b>Buckling coefficient</b>		<b>22.98</b>	

**Table 3.** Verification results of work condition 2

Component	Normal stress / (MPa)	Shearing stress / (MPa)	Displacement / (mm)
vertical rib	151.6	0.41	0.31
horizontal brace	115.7	4.6	0.31
inter-support (beam)	36.7	21.0	0.36
inter-support (truss)	65.3	6.0	50.3
<b>Maximum displacement</b>		<b>50.5 cm</b>	
<b>Buckling coefficient</b>		<b>22.98</b>	

**Table 4.** Verification results of work condition 3

Component	Normal stress / (MPa)	Shearing stress / (MPa)	Displacement / (mm)
vertical rib	147.6	0.4	4.0
horizontal brace	108.1	5.1	5.5
inter-support (beam)	37.9	21.9	4.0
inter-support (truss)	90.8	6.1	50.2
<b>Maximum displacement</b>		<b>50.5 cm</b>	
<b>Buckling coefficient</b>		<b>22.98</b>	
<b>Anti-floating coefficient</b>		<b>1.65</b>	
<b>Anti-sliding coefficient</b>		<b>1.37</b>	

**Fig. 6.** Displacement cloud map of conditions 1, 2, & 3.

In summary, the construction plan of the first cofferdam and then the pile has sufficient safety.

## 4 Large-Volume Concrete Temperature Control Technology

### 4.1 Construction Method

The Longshan Bridge has 5 main piers, with similar structural forms. The dimensions of the pier caps are  $23.48\text{m} \times 19.98\text{m}$ , with  $1.458 \times 1.458\text{m}$  chamfers at the four corners. The pier cap is 4 meters thick, and the bottom concrete is 5 meters thick. The elevation of the bottom and the top of the pier cap are 144.5m and 153.5m respectively. The total volume of concrete for a single pier cap is  $4939\text{m}^3$ .

The height of the pile is 4.0 meters, and concrete pouring is carried out in two 2.0-meter layers. After pouring concrete, pre-embedded cooling water pipes can cool down the concrete by passing water through it. There are 4 layers of cooling water pipes. The top layer of cooling water pipes keeps 50cm away from the top surface. The vertical spacing between each layer is 100cm, and the distribution plan for cold water pipes is shown in Fig. 7.

To reduce shrinkage cracks and make the concrete surface more beautiful, after the top layer of concrete is poured, a secondary compaction and leveling operation is carried out. Then, cover the concrete with geotextile and sprinkle water for curing, while setting up a cooling shed. Once the strength of the concrete attaches to 2.5MPa, the template can be dismantled.

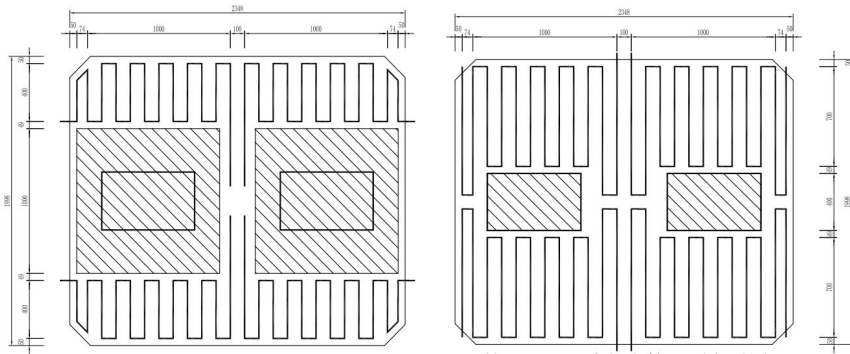


**Fig. 7.** Layout of water pipes (the first and second floors above, and the third and fourth floors below)

To reduce hydration heat, make large-volume concrete have excellent corrosion resistance, volume stability, crack resistance, low hydration heat, and low alkaline content cement. When adding ground slag alone, the dosage should not be less than 50%. Meanwhile, it is suitable to use fly ash with silica fume, fly ash with slag, or more mineral admixtures to reduce heat generation.

## 4.2 Hydration Heat Analysis

The hydration heat of cement can be calculated according to equation (1) [10], that is:

$$Q(t) = Q_0 (1 - e^{-at^b}) \quad (1)$$

where  $Q(t)$  is the hydration heat of cement,  $Q_0$  is the maximum hydration heat index,  $t$  is the hydration time (cement age), and  $a$  and  $b$  are two material parameters.

The adiabatic heating can be approximately determined according to equation (2), that is:

$$T(t) = \frac{WQ}{c\rho} (1 - e^{-mt}) \quad (2)$$

where  $T(t)$  is the adiabatic heating of concrete,  $W$  is the total amount of cementitious material used,  $c$  is the specific heat of concrete,  $\rho$  is the density of concrete, and  $m$  is the cement correction parameter.

The parameter  $m$  can be determined by Eq. (3).

$$m = k(A\lambda W_c + B) \quad (3)$$

where,  $W_c$  is the amount of Portland cement used per cubic meter of concrete, and  $\lambda$  is the correction factor.  $k$  is the reduction factor for the admixture, and  $A$  and  $B$  are the temperature adjustment factors for molding. For slag Portland cement (P·S·A), the parameter  $\lambda$  can be taken as 0.65, and for slag, the parameter  $k$  can be taken as 0.25.

The concrete mix proportions and corresponding thermal parameters of each material are shown in Tables 5 and 6.

**Table 5.** Selected concrete mix ratio (kg/m<sup>3</sup>)

Mark	Cement	Fly ash	Sand	Gravel	Water	Admixture
C30	312	78	810	1075	175	3.9
C40	315	135	679	1109	162	4.5

**Table 6.** Percentage of concrete and thermal parameters of raw materials

Raw material	Percentage Content / (%)		Specific heat kJ/(kg·°C)	Thermal conductivity coefficient kJ/(kg·h·°C)
	C30	C40		
Cement	12.71	13.10	0.46	4.45
Fly ash	3.18	5.61	0.92	0.83
Sand	33.01	28.24	0.70	11.13
Gravel	43.81	46.12	0.72	10.51
Water	7.13	6.74	4.19	2.16
Admixture	0.16	0.19	0.92	0.83

According to the homogenization (weighted average by mass) method, the densities of C30 and C40 concrete are  $2453.9\text{kg/m}^3$  and  $2404.5\text{ kg/m}^3$ , and their thermal conductivity coefficient of them is  $9.03\text{ kJ}/(\text{kg}\cdot\text{h}\cdot^\circ\text{C})$  and  $8.77\text{ kJ}/(\text{kg}\cdot\text{h}\cdot^\circ\text{C})$  respectively. Meanwhile, the specific heat of both C30 and C40 concrete is  $0.93\text{ kJ}/(\text{kg}\cdot^\circ\text{C})$ .

Based on the dimensions and cooling water pipe layout in Fig 9, a model was established in the FEM software Midas/FEA for the hydration heat simulation, which is shown in Fig 8.

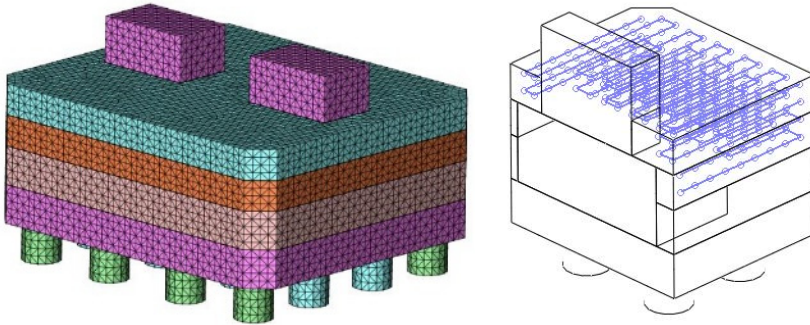


**Fig. 8.** Numerical model for hydration heat calculation

The model shown in Fig. 8 consists of 41432 units and 219228 nodes, in which the cooling water pipes are inserted in the form of pipe units. The calculation parameters for the cooling water pipes are shown in Table 7.

**Table 7.** Parameters for cooling water pipes

Diameter mm	convection coefficient $\text{m}^2\cdot^\circ\text{C}$	Specific heat $\text{kJ}/(\text{kg}\cdot^\circ\text{C})$	Inlet temperature $^\circ\text{C}$	flow rate $\text{m}^3/\text{h}$
42	272	4.2	25	1.5

Taking the noncooling water condition as an example, at the most disadvantage moment, the cloud map of the temperature inside the model is shown in Fig. 4. The highest temperature inside the concrete can attach to  $69\text{ }^\circ\text{C}$ , which accords to the maximum temperature requirements for code.

Meanwhile, the simulated temperature stress results (maximum stress history curve) under noncooling water conditions and water-cooling operating conditions are calculated. During the cooling water passing through, the stress development curve of the concrete bearing platform is within the allowable stress development curve range. Therefore, there should be no temperature cracks in theory analysis, and the cooling measures proposed in this article are effective.

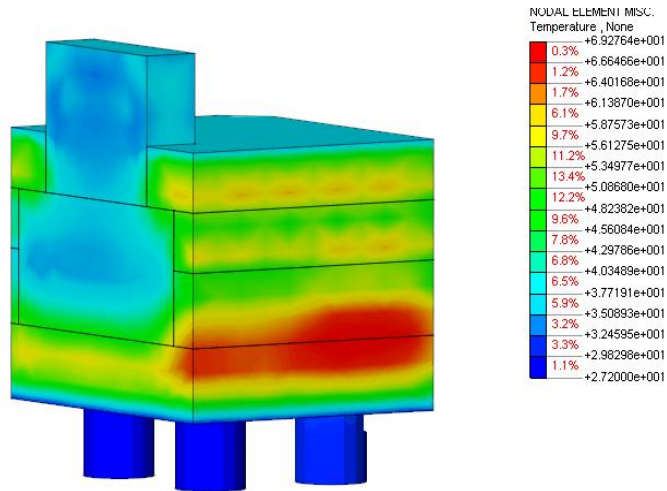


Fig. 9. Cloud map of maximum temperature of concrete

## 5 Conclusions

In this study, the construction scheme for the large volume bearing platform of Longshan Bridge was introduced. In terms of the cofferdam construction plan and temperature control measures, numerical simulations were conducted. Based on the engineering, two construction experiences were summarized:

(1) Compared to the scheme of the first cofferdam and then pile, the first pile and then cofferdam scheme is more effective, and in section 2, a specific plan has been provided, which can be used as a reference for similar projects.

(2) Reducing the heat of hydration will give large-volume concrete good corrosion resistance, volume stability, and crack resistance. In this engineering, cement with low heat of hydration and low alkaline content is selected, and a water-cooling system is installed, which is also a good engineering reference.

## Acknowledgments

This work was financially supported by the National Natural Science Foundation of China (CN) (Grant Nos. 41772308) and the Science Foundation of Hubei Road Co. Ltd.

## References

1. Ma X, Sun Q, Li Z, et al. Deformation and internal force of multitower suspension bridges: Numerical modeling and analytical analysis[J]. *Advances in Structural Engineering*, 2025, 28(5): 811-827.

2. Wang R, Zhou G, Zuo X. Test and numerical study on blast resistance of main girders coated with polyurea in self-anchored suspension bridges[J]. Applied Sciences, 2024, 14(20): 14209280.
3. Xue D, Liu J, Song Y, et al. Performance analysis of a hybrid dehumidification system adapted for suspension bridge corrosion protection: a numerical study[J]. Applied Sciences, 2023, 13(7): 13074219.
4. Fan Y, Zhou J, Luo C, et al. Research on loading scheme for large-scale model tests of the super-long-span arch bridge [J]. Buildings, 2023, 13(7): 1639.
5. Nan L, Yang Q, Liu Y, et al. Application of long-span continuous bridge technology in bridge construction[J]. Journal of Architectural Research and Development, 2023, 7(3): 7-12.
6. Zhu H, Zhang X. Floating stability analysis of steel boxed cofferdam of Dongtinghu long-span bridge [J]. Applied Mechanics and Materials, 2013, 2659(395&396): 897-900.
7. Wang T, Liang H, Peng Z. Numerical simulation on offshore artificial island cofferdam of Hong Kong-Zhuhai-Macao bridge [J]. International Journal of Computer Applications in Technology, 2020, 64(4): 285-295.
8. Aleksandra K, Krzysztof W. FEM and experimental investigations of concrete temperature field in the massive stem wall of the bridge abutment [J]. Construction and Building Materials, 2022, 347: 128565.
9. Rodrigo A. High temperature and cracking: equations to avoid high-heat concrete mixtures in massive bridge footings [J]. Journal of Materials in Civil Engineering, 2021, 33(12).
10. Huang Y, Liu G, Huang S, et al. Experimental and finite element investigations on the temperature field of a massive bridge pier caused by the hydration heat of concrete [J]. Construction and Building Materials, 2018, 192: 240-252.

**Open Access** This chapter is licensed under the terms of the Creative Commons Attribution-NonCommercial 4.0 International License (<http://creativecommons.org/licenses/by-nc/4.0/>), which permits any noncommercial use, sharing, adaptation, distribution and reproduction in any medium or format, as long as you give appropriate credit to the original author(s) and the source, provide a link to the Creative Commons license and indicate if changes were made.

The images or other third party material in this chapter are included in the chapter's Creative Commons license, unless indicated otherwise in a credit line to the material. If material is not included in the chapter's Creative Commons license and your intended use is not permitted by statutory regulation or exceeds the permitted use, you will need to obtain permission directly from the copyright holder.

